water

MDPI

Article

Cascading Failure and Resilience of Urban Rail Transit Stations under Flood Conditions: A Case Study of Shanghai Metro

Dekui Li [1,*], Yuru Hou [1], Shubo Du [2] and Fan Zhou [1,*]

[1] School of Computer Science, Liaocheng University, Liaocheng 252000, China; hyr018@163.com
[2] School of Architecture, Liaocheng University, Liaocheng 252000, China; dushubo@tongji.edu.cn
* Correspondence: jerryinkorea@gmail.com (D.L.); zhoufan@lcu-cs.com (F.Z.); Tel.: +86-18063512250 (D.L.); +86-15266816303 (F.Z.)

Abstract: The increasing frequency of urban flooding, driven by global climate change, poses significant threats to the safety and resilience of urban rail transit systems. This study systematically examines the cascading failure processes and resilience of these networks under flood conditions, with a specific focus on the Shanghai Metro. A comprehensive resilience evaluation model was developed by integrating geographic information, static network characteristics, and dynamic passenger flow indicators. This study employs an improved Coupled Map Lattice (CML) model to simulate cascading failures by considering the coupling effects of station centrality, geographic elevation, and passenger flow dynamics. The results indicate that stations with higher degrees of centrality are more likely to trigger rapid cascading failures across the network. However, incorporating dynamic passenger flow and geographic elevation data helps mitigate these effects, emphasizing the need for multi-dimensional resilience strategies. The findings provide valuable insights for urban transit management, offering a scientific foundation for developing targeted disaster response strategies to enhance network resilience against floods. This study advances our understanding of the vulnerability of urban rail transit systems and offers practical guidance for improving disaster preparedness in urban transportation infrastructure.

Keywords: cascading failure; urban rail transit; resilience; flood; Coupled Map Lattice (CML) model

Citation: Li, D.; Hou, Y.; Du, S.; Zhou, F. Cascading Failure and Resilience of Urban Rail Transit Stations under Flood Conditions: A Case Study of Shanghai Metro. *Water* **2024**, *16*, 2731. https://doi.org/10.3390/w16192731

Academic Editors: Weiwei Shao, Zhaohui Yang and Xichao Gao

Received: 16 August 2024
Revised: 22 September 2024
Accepted: 24 September 2024
Published: 25 September 2024

1. Introduction

Urban rail transit systems are essential components of modern cities, facilitating the daily movement of millions of passengers. However, these systems are increasingly vulnerable to disruptions caused by extreme weather events, particularly urban flooding. Flooding poses significant risks to urban rail transit systems, especially those characterized by enclosed spaces, high passenger density, and extensive underground infrastructure. Historical incidents provide clear evidence of this vulnerability. For instance, the nation's busiest subway system in New York sustained the severest damage in its 108 years of operation due to Hurricane Sandy on 29 October 2012. The storm left millions of people without service for at least a week and caused significant disruptions to transit infrastructure [1]. Similarly, the catastrophic flooding of the Zhengzhou Metro in 2021, which resulted in multiple fatalities, underscores the critical need for resilience in these networks [2]. Such events demonstrate the potential for cascading failures, where the disruption of a single station can propagate throughout the entire network, leading to widespread service interruptions, economic losses, and threats to public safety.

Existing research on the resilience of transportation networks often focuses on static network indicators and risk assessments. For instance, Bo et al. developed a vulnerability assessment system for bus networks under heavy rain and flooding, incorporating both static network characteristics and dynamic passenger flow indicators [3]. Similarly, Wang et al. utilized the Fuzzy Analytic Hierarchy Process (FAHP) to construct specific indicators

for assessing the flood risk of the Beijing Metro by integrating disaster environment factors, disaster-inducing factors, and the characteristics of disaster-bearing bodies [4]. Li et al. applied complex network theory to model the evolution of disaster chains in urban rail transit triggered by floods [5].

However, there remains a significant gap regarding the dynamic interactions between geographic factors, network topology, and real-time passenger flow during flood events [6]. While some studies, such as Kim et al.'s, emphasize the role of smart city technologies in mitigating disaster risks through data analysis and automation [7], few studies fully explore the dynamic nature of cascading failures in urban rail systems. Catelani et al. provided insights into improving the maintainability of railway systems through the allocation of maintenance resources based on failure rates, yet further research is needed to link these insights to flood-induced cascading failures [8].

In terms of disaster communication, Khaliq et al. proposed an emergency response system using vehicular networks, which ensures communication during disasters, even when traditional networks fail [9]. Similarly, Kumsap et al. developed a mesh communication backbone for disaster management, demonstrating that effective communication infrastructure can significantly improve disaster response efforts [10].

Moreover, digital post-disaster risk management techniques are critical for enhancing urban resilience. Lagap and Ghaffarian proposed an improved framework for digital twinning and real-time monitoring, underscoring the importance of using digital technologies, such as IoT, AI, and big data analytics, for post-disaster recovery [11]. Lastly, De Francesco and Leccese analyzed the risks to electric lifelines during seismic disasters and proposed strategies for the recovery and maintenance of critical infrastructure [12].

This study addresses these gaps by systematically analyzing the cascading failure mechanisms of urban rail transit systems under flood conditions, with a focus on the Shanghai Metro. By integrating geographic information systems (GIS), complex network theory, and dynamic passenger flow data, this research seeks to develop a robust framework for evaluating the resilience of rail transit networks. The inclusion of three-dimensional geographic information and time-varying passenger flow dynamics offers a more comprehensive understanding of how urban flooding impacts network resilience while also exploring variations in resilience under different flood scenarios.

By integrating insights from the aforementioned international studies, this research significantly advances the development of robust disaster response strategies, thereby strengthening the resilience of urban rail systems in the face of flood-induced disruptions. This broader incorporation of global research not only enhances the capacity of these systems to withstand and recover from extreme events but also bridges the gap between theoretical frameworks and practical implementations. As a result, this study offers critical contributions to both academic discourse and the formulation of real-world disaster management practices.

2. Evaluation Indicators for the Resilience of Rail Transit Networks under Flood Conditions

2.1. Rail Transit Network Characteristics

Among the various methods for constructing these networks, the Space L and Space P methods are commonly employed [13]. Given that this study emphasizes the spatial characteristics of rail transit networks within an urban geographic context, the Space L method is selected for network construction.

In the context of rail transit network resilience, the degree of centrality is a pivotal factor in determining the likelihood and impact of cascading failures [14]. Previous studies have examined the characteristics of the Shanghai rail transit network from a complex network perspective, confirming that the network exhibits small-world and scale-free properties. These characteristics render the network particularly susceptible to targeted attacks on nodes with a high degree of centrality [15,16]. Furthermore, cascading failures in the Chengdu Metro have been studied, showing that transfer stations, due to their central

role and high passenger flow, experience greater failure scales and exert a more significant impact on the overall network when they are disrupted [17].

This study utilizes the degree of centrality as the primary network characteristic indicator for analyzing node importance. Figure 1 illustrates the impact on the network following the failure of stations with varying degrees of centrality. Station A, with a degree of centrality of 5, functions as a crucial transfer point within the network, affecting five other stations when it fails. In contrast, Station B, with a lower degree of centrality of 2, primarily connects to two other stations, and its failure has a correspondingly smaller impact.

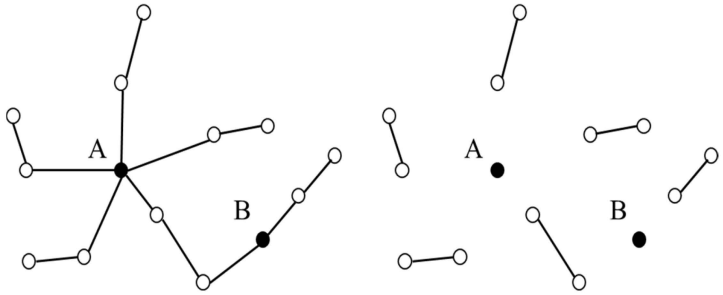

Figure 1. Impact on the network after the destruction of stations with varying degrees of centrality.

2.2. Geographic Information of Stations

Existing studies on the resilience assessment of urban rail transit networks have largely focused on static network characteristics and two-dimensional analyses, thus lacking a comprehensive, multi-dimensional, and dynamic approach to network resilience [18]. The impact of urban flooding on rail transit systems is uniquely challenging, posing significant threats to the resilience of the entire network. Urban floods typically disperse according to the city's spatial layout, interacting with the three-dimensional (3D) network structure of roads and railways and thereby influencing the entire transit network [19]. This mode of impact differs significantly from those caused by deliberate sabotage or random failures. Flood-induced disruptions in rail transit are heavily influenced by geographic factors, where localized network interruptions can lead to widespread effects across areas indirectly affected by the flood.

Current research on transportation networks largely relies on two-dimensional (2D) complex networks using geographic coordinates, with a limited focus on 3D network topology and the dynamic effects of geographic elevation [20]. However, existing and complex network-based frameworks for analyzing transportation under flood conditions are not well-suited to accounting for 3D disturbances and topologies. The inclusion of geographic elevation as a critical third dimension is essential for accurately assessing the impacts of floods on transit networks [6]. As illustrated in Figure 2, when stations A and B are damaged by flooding, the elevation of neighboring stations plays a significant role in influencing the cascading failure effect across the network.

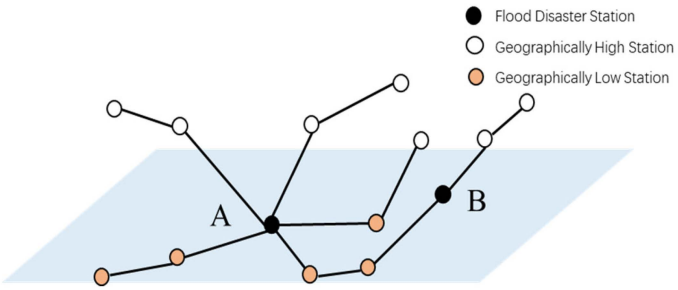

Figure 2. Impact of stations at different elevations under flood conditions.

2.3. Stations' Dynamic Characteristics of Passenger Flow

In the study of cascading failures within urban rail transit networks, changes in passenger flow are considered critical indicators. Chen et al. utilized Automatic Fare Collection (AFC) data from the Beijing Metro to construct an Origin–Destination (OD) matrix for passenger flow by applying an all-or-nothing assignment based on the shortest path. They assessed the reliability of the Beijing Metro network with and without passenger flow weighting, concluding that the network is more vulnerable when passenger flow is factored into the analysis [21]. Similarly, Liu et al. employed the Floyd algorithm to calculate the shortest path from the origin to the destination, assuming that when a node fails, its passenger flow automatically redirects to the nearest alternative path until no further nodes fail [22]. Their model primarily addresses congestion failures caused by the failure of specific nodes.

Moreover, Huang et al. used the Coupled Map Lattice (CML) model, incorporating passenger flow as a weighted parameter, to construct a stability analysis model for the passenger-flow-weighted complex network in 2014 and 2018, to analyze the stability evolution of the Beijing Metro network [23]. Zhu et al. developed a passenger-flow-weighted reliability evaluation index using AFC data from the Shanghai Metro and employed the Dijkstra shortest path algorithm to determine the passenger flow weight of network nodes. They built a dynamic model of the Shanghai rail transit network based on the CML model and conducted a comprehensive network reliability analysis [24]. However, these studies often consider passenger flow as a static weighting indicator for nodes, which does not fully capture the dynamic impacts of passenger flow fluctuations across the entire network due to station failures.

In the event of a real flood disaster, the failure of a rail transit station can lead to two primary scenarios: one where the station is closed and trains bypass the station, causing passengers to alight at the preceding or subsequent stations, and another where the train halts at the previous station and resumes service only after the affected station is cleared for safety. The likelihood of passengers continuing to search for the shortest path within the disrupted rail transit system is minimal. Therefore, this study constructs a dynamic matrix of station passenger volume based on time-varying AFC data, thus establishing dynamic weighting indicators for passenger flow. This approach is then utilized to calculate the cascading failure effects on the dynamic impact of network passenger capacity following station failures due to flood conditions.

3. Modeling and Analysis of Cascading Failures in Rail Transit Networks Based on CML

3.1. Coupled Map Lattice (CML)

Current research on cascading failures in networks primarily utilizes complex network models, load-capacity models, and Coupled Map Lattice models [25]. The Coupled Map Lattice (CML) model discretizes time and space variables while keeping state variables continuous. It reflects the degree of chaos at nodes and the diffusion effects of cascading failure processes within the system, making it suitable for analyzing the spatiotemporal dynamics and patterns of networks [26]. This study employs the CML model to investigate cascading failures in rail transit networks.

The selection of the CML model for this study is primarily motivated by its capacity to capture dynamic interactions within complex networks, particularly under spatiotemporal disruptions, such as flooding. Unlike traditional approaches, the CML model offers several distinct advantages. For instance, complex network models typically emphasize static network properties, such as the degree of centrality, but fall short in representing the dynamic behavior of nodes during cascading failures. Similarly, load-capacity models, while useful in assessing failures based on predefined thresholds, do not account for the continuous evolution of node states and changes in network topology over time [25].

In contrast, the CML model excels in discretizing both time and space while simultaneously allowing for the continuous variation of state variables. This makes it especially well-suited to analyzing the spatiotemporal dynamics of urban rail networks under condi-

tions of flooding. The model effectively simulates how disruptions at one station propagate throughout the network, thus integrating geographic factors and dynamic passenger flows [26]. By incorporating real-time variations in passenger behavior, geographical elevation, and network topology, the CML model delivers a more comprehensive framework for understanding cascading failures within urban rail transit systems [27].

Although other models, such as agent-based simulations or flow-redistribution models, might also be applicable, they often lack the precision required to capture the chaotic interactions between stations during failures. The CML model's robustness in modeling these complex dynamics justifies its use in this research. Moreover, previous studies, such as those by Huang et al. and Liu et al., have demonstrated the effectiveness of CML in simulating cascading failures within urban rail networks, further affirming the model's relevance and utility in this context [23,24].

In real-world scenarios, when a rail transit station is affected by flooding, the failure of the station could be caused by its geographic characteristics, changes in the overall network topology, or dynamic variations in passenger flow. Subsequently, both the network topology and the flow distribution within the entire rail transit system are affected, leading to the sequential failure of stations due to the combined effects of the "geographically weighted topological network" and the "dynamic passenger flow network". In essence, the "dynamic passenger flow network" is a result of the dynamic changes in passenger flow triggered by the failure of the topological network.

Therefore, considering the impact of dynamic passenger behavior on network resilience in reality, this study incorporates actual passenger flow data into the geographically weighted topological network of rail transit stations. By analyzing the behavior of cascading failures in the entire rail transit system under different coupling strengths of these two networks, this research has significant implications for improving the resilience of actual rail transit networks. The formula commonly used in CML for networks is as follows in Equation (1):

$$\begin{gathered} x_i(t+1) = \left| (1-\varepsilon) f(x_i(t)) + \varepsilon \sum_{j=1, j\neq i}^{n} \frac{a_{ij} f\left(x_j(t)\right)}{k_i} \right| \\ k(i) = \sum_{j \in n} a_{ij} \\ f(x) = 4x(1-x) \end{gathered} \tag{1}$$

In the formula, $x_i(t)$ represents the CML state of node i at time t, ε is the coupling coefficient introduced for the unweighted topological network, and k_i denotes the degree of node i, which refers to the number of other nodes directly connected to it. a_{ij} is the element in the adjacency matrix corresponding to the i row and the j column, and $f(x)$ is a nonlinear mapping function, which can be physically interpreted as the evolution of node i's capacity or operational constraints, with a value range between (0 and 1).

This study uses the enhanced Coupled Map Lattice model proposed by Huang et al. [23] and Shen et al. [27], as shown in Equation (2).

$$\begin{gathered} x_i(t+1) = \left| \begin{array}{c} (1-\varepsilon_{dr}-\varepsilon_{de}-\varepsilon_{in}-\varepsilon_{out}) f(x_i(t)) + \varepsilon_{dr} \sum\limits_{j,j\neq i} a_{ij} \dfrac{f\left(x_j(t)\right)}{k_i} + \varepsilon_{de} d_i \dfrac{f(x_i(t))}{} \\ + \varepsilon_{in} \sum\limits_{j,j\neq i} s_i^{in} \dfrac{f(x_i(t))}{w_{ij}^{in}} + \varepsilon_{out} \sum\limits_{j,j\neq i} s_i^{out} \dfrac{f(x_i(t))}{w_{ij}^{out}} \end{array} \right| + R \\ \varepsilon_{dr}, \varepsilon_{de}, \varepsilon_{in}, \varepsilon_{out} \in (0,1) \\ \varepsilon_{dr} + \varepsilon_{de} + \varepsilon_{in} + \varepsilon_{out} \leq 1 \end{gathered} \tag{2}$$

ε_{dr} is the coupling coefficient introduced for the unweighted topological network, ε_{de} is the deep coupling coefficient, and ε_{in} ε_{out} is the coupling coefficient for the weighted distribution of inflow and outflow at the stations, which, respectively, represent the differences in network coupling relations caused by the presence or absence of depth and the loading of flow.

a_{ij} indicates the connection status between node i and node j. If there is an edge connecting nodes i and j, then $a_{ij} = a_{ji} = 1$; otherwise, $a_{ij} = a_{ji} = 0$. k_i is the degree of node i, d_i i is the depth-normalized value of the node, s_i^{in} represents the inflow strength at node i, s_i^{out} represents the outflow strength at node i, w_{ij}^{in} represents the inflow strength at other nodes, and w_{ij}^{out} represents the outflow strength at other nodes. R represents the perturbation intensity.

3.2. Spatiotemporal State of Network Stations under Different Conditions

The CML model describes the state of network nodes and their interactions. At each time step, the state of a particular node is influenced by its state at the previous time step and the states of surrounding nodes. Initially, at time $t = 0$, each node is randomly assigned a value between 0 and 1. At the next time, step $t = 1$, a new state value is calculated according to Equation (1). Over time, the CML values of network nodes across all time steps are obtained. When the network is not disturbed, the node states remain within the range of 0 to 1. Taking Station 45 of the Shanghai rail transit as an example, its CML state without applying any disturbance R is shown in Figure 3.

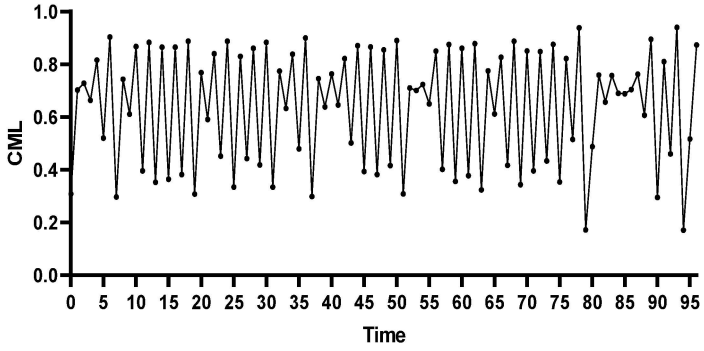

Figure 3. CML state of station 45 (without disturbance).

This study employs an improved Coupled Map Lattice (CML) model to simulate cascading failures while considering the coupling effects of station centrality, geographic elevation, passenger flow dynamics, and passenger behavior. Chen et al. introduced coupling coefficients to reflect the influence of station centrality and network topology on failure propagation, highlighting that stations with higher passenger flows and greater centrality were more likely to trigger network-wide failures [21]. Ma et al. also emphasized that passenger boarding and alighting behaviors play a critical role in influencing failure propagation [28]. Therefore, we incorporated these behaviors as part of the coupling coefficients in our study. Liu et al. further analyzed the resilience of urban rail transit networks to cascading failures, identifying that a coupling coefficient of 0.5 could trigger noticeable cascading failures [22]. Based on these findings, we employed a total coupling coefficient of 0.5 by summing the station centrality, depth coefficient, and passenger flow coefficients and by incorporating passenger behavior to enhance the model's accuracy under flood conditions.

When a node in the network is disturbed at a certain time t ($R \geq 1$), this node fails and is removed from the network at the next time, step $t + 1$. The neighboring nodes of this failed node are affected, potentially leading to their failure and causing the failure to propagate to adjacent nodes until no more nodes fail, at which point the cascading failure in the network stops. According to Equation (2), different coupling coefficients result in different states, thus affecting the speed and extent of the failure. Taking Station 45 as an example, with external disturbance R = 1 applied at time step 27, the CML state under different combinations of coupling coefficients (Combination 1: $\varepsilon_{dr} = 0.5$; Combination 2: $\varepsilon_{dr} = 0.3$, $\varepsilon_{in} = 0.1$, $\varepsilon_{out} = 0.1$; Combination 3: $\varepsilon_{dr} = 0.3$, $\varepsilon_{de} = 0.2$, $\varepsilon_{in} = 0.05$, $\varepsilon_{out} = 0.05$) is shown in Figure 4.

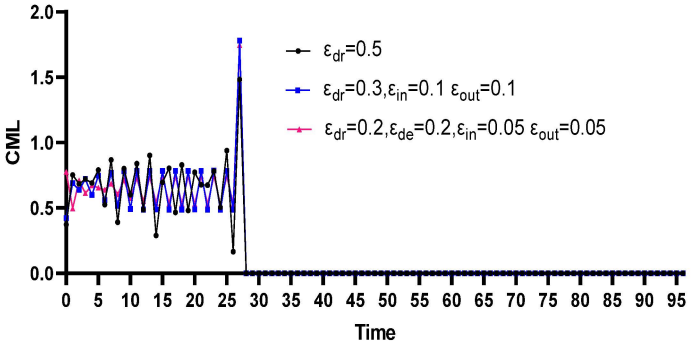

Figure 4. CML state of Station 45 under different coupling coefficients.

When a node in the network is disturbed at a certain time, t, it can trigger cascading failures throughout the network. The effect of cascading failures varies under different disturbances. Taking Station 45 as an example, with external disturbances R = 1, 2, 3, 4, 5, 6 applied at time step 27, and with the coupling coefficients set to Combination 1, $\varepsilon_{dr} = 0.5$, the cascading failure effect on other nodes in the network is shown in Figure 5. As R increases, the number of failed nodes increases, and the failure speed accelerates. Due to the cascading failures in the network, the impact on passenger flow is illustrated in Figure 6, where the number of affected passengers increases with higher values of R.

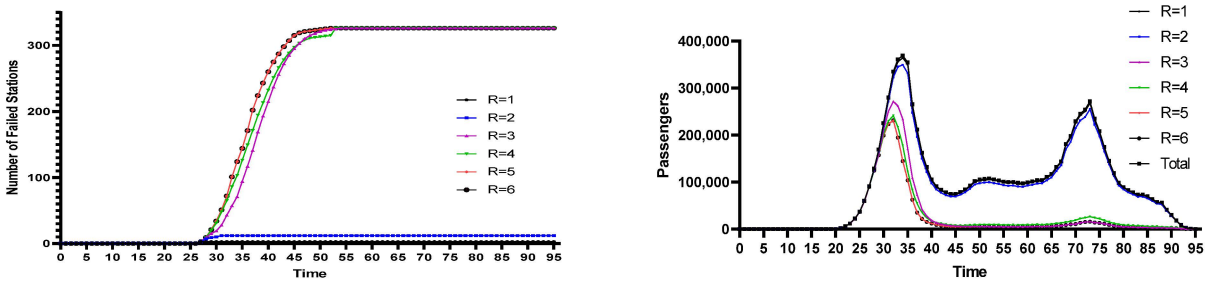

(**a**) (**b**)

Figure 5. (**a**) Condition of failed stations at Station 45 under different disturbances. (**b**) Impact on passenger flow at Station 45 under different disturbances.

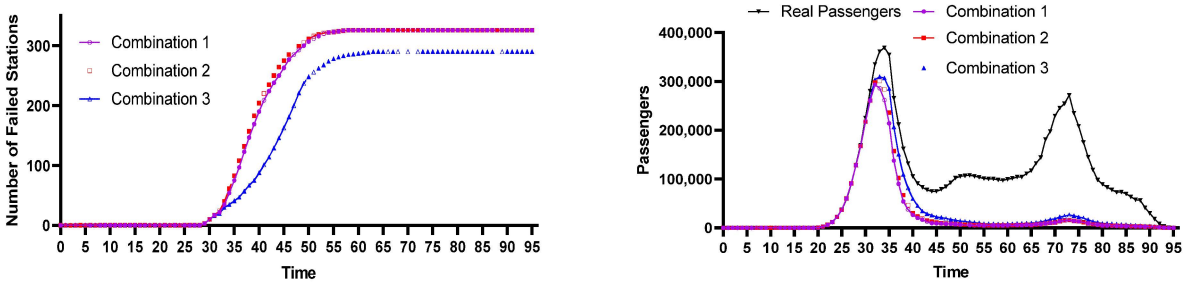

(**a**) (**b**)

Figure 6. (**a**) Cascading failure process under different coupling coefficients of Station 41. (**b**) Passenger flow changes under different coupling coefficients of Station 41.

3.3. Resilience Algorithm Process for Cascading Failures in Rail Transit Based on CML

The CML state values of network stations, the number of failed nodes, the geographically weighted topological network, and the stability of the dynamic passenger flow network at different time points during the cascading failure process can be obtained through the following algorithmic process:

Step 1: Determine the initial values by calculating the network centrality, geographic weighted intensity, and passenger flow weighted intensity of each station, and set the CML state values for all stations in the network.

Step 2: Select a specific time point and deliberately disturb the stations with the highest degree of centrality, stations at lower geographic elevations, and stations historically affected by flooding to cause failure. Record the attribute values at the current time point.

Step 3: Assess the CML state values of all stations from the previous time point. If the state value $x_i(t) \geq 1$, the station is considered to have failed, and it is removed from the network. Update the CML state values for the remaining network stations and record the attribute values at the current time point.

Step 4: Repeat Step 3 until the number of failed stations in the network no longer changes. The network reaches a new stable state, and the new attribute values are recorded.

Step 5: Repeat Steps 2 through 4, output the results for each time point, and record the corresponding statistical data.

4. Results of Cascading Failure Process and Resilience Analysis of the Shanghai Rail Transit Network under Flood Conditions

4.1. Data Source

Due to the varied sources of data, this study maximizes the use of data from the same time period.

Passenger Flow Data: Based on the Shanghai Metro AFC (Automatic Fare Collection) card data publicly available through the Shanghai Open Data Applications (SODA) competition, data from Tuesday, 8 March 2016 were used. After cleaning the data, a 15 min interval was adopted, with 96 time steps recorded from 00:00 to 24:00 as the basis for time and passenger statistics.

Metro Station Data: By the end of 2016, the Shanghai Metro had 14 lines with a total of 326 stations.

Station Elevation Data: Elevation data for Shanghai Metro stations were obtained using the publicly available 50 m DEM (Digital Elevation Model) data from the Geospatial Data Cloud. Only the gravitational influence on water flow direction was considered. The ArcGIS Hydrology Analysis module was used to generate a flow direction map and extract catchment basins. Combined with the raster data of Shanghai Metro stations, the depth information of metro stations was extracted. For stations without catchment basin information, the DEM elevation data were directly used [29].

4.2. Analysis of Stepwise Weighted Resilience Changes during the Cascading Failure Process of the Rail Transit Network under Flood Conditions

The initial values were determined by calculating the network centrality, geographic weighted height, and passenger-flow-weighted intensity for each station and subsequently setting the CML state values across the entire network. In this study, three stations with the highest degree of centrality, three stations at lower geographic elevations, and three stations with a history of flood damage were selected. The disturbances were introduced starting at 7:00 AM, corresponding to the 29th time step.

4.2.1. Stations with the Highest Degree of Centrality

Stations with higher degrees of centrality are more important within the network. In a metro network, stations with high degree values are often located in central areas of the network, while those with lower values are usually on the periphery. To study the impact of stations with different degree values on the cascading failure process of the network, three metro stations were selected: Shanghai Rail Transit Station 41 (degree of centrality 7, depth 0.96), Station 19 (degree of centrality 6, depth 0.96), and Station 45 (degree of centrality 6, depth 0.93). Under different combinations of coupling coefficients (Combination 1: $\varepsilon_{dr} = 0.5$; Combination 2: $\varepsilon_{dr} = 0.3$, $\varepsilon_{in} = 0.1$, $\varepsilon_{out} = 0.1$; Combination 3: $\varepsilon_{dr} = 0.3$, $\varepsilon_{de} = 0.2$, $\varepsilon_{in} = 0.05$, $\varepsilon_{out} = 0.05$), the same disturbance, R = 4, was applied. The

resulting network station failure process, the number of failures, and changes in passenger flow are shown in Figures 6–8.

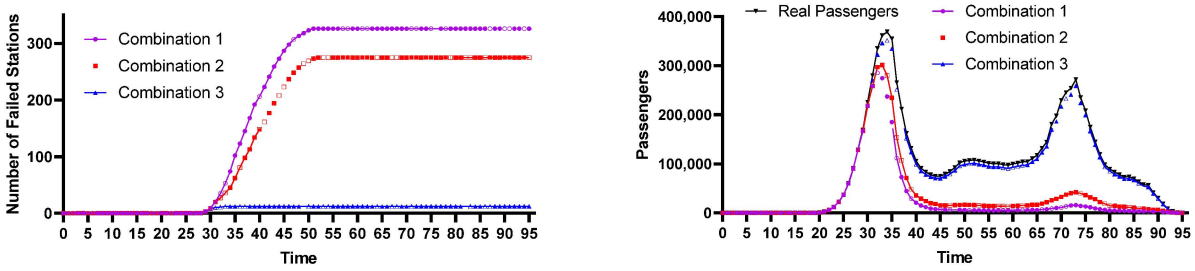

(**a**) (**b**)

Figure 7. (**a**) Cascading failure process under different coupling coefficients of Station 19. (**b**) Passenger flow changes under different coupling coefficients of Station 19.

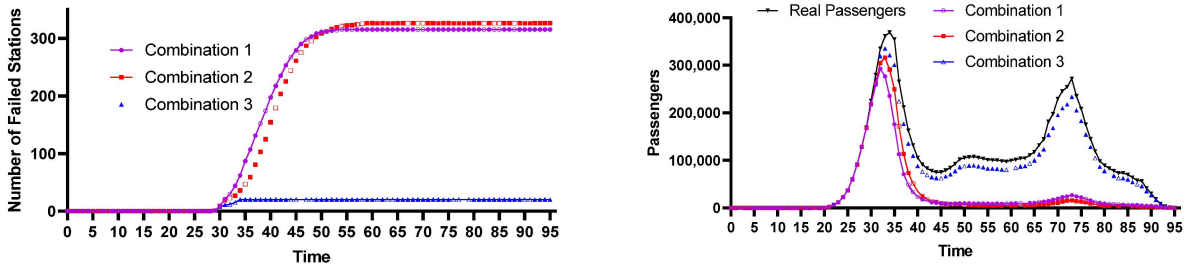

(**a**) (**b**)

Figure 8. (**a**) Cascading failure process under different coupling coefficients of Station 45. (**b**) Passenger flow changes under different coupling coefficients of Station 45.

Stations with high degrees of centrality are often more important stations, and the overall network damage process varies with different coupling coefficients. Among the 41 stations, when the passenger flow coefficient is added (Combination 2), the entire network's damage rate increases. When both the passenger flow and the depth coefficients are added (Combination 3), the network's damage rate slows down, and some stations remain undamaged at R = 4 (Figure 6a). However, from the perspective of passenger flow, if the damage begins at 7 a.m., after the morning peak, the passenger flow is significantly affected (Figure 6b).

Among the 19 stations, when the passenger flow coefficient is added (Combination 2), the overall network damage rate decreases, and some nodes remain undamaged at R = 4. When both the passenger flow and depth coefficients are added (Combination 3), the overall network damage is reduced, with only a dozen nodes being destroyed (Figure 7a), and the affected passenger flow is minimal (Figure 7b).

In the experiment with 45 stations, adding the passenger flow coefficient (Combination 2) slows down the network damage compared to when only the degree of centrality is considered, but the number of damaged stations increases (Figure 8a). When both the passenger flow and depth coefficients are added (Combination 3), similarly to the 19 stations, the overall network damage is reduced, with only a dozen stations being destroyed, and the impact on passenger flow is minimal (Figure 8b).

4.2.2. Centrality of Stations with Lower Geographical Positions

The lower the geographical elevation of a station, the more important it becomes to the network during flood disasters. To study the impact of stations at different depths on the network's cascading failure process, three subway stations in Shanghai's rail transit system were selected: Station 159 (degree of centrality 4, depth 0.99), Station 164 (degree

of centrality 4, depth 0.99), and Station 189 (degree of centrality 4, depth 0.99). The same disturbance, R = 4, was applied under different coupling coefficient combinations, and the resulting network station damage process and reliability changes are shown in Figures 9–11.

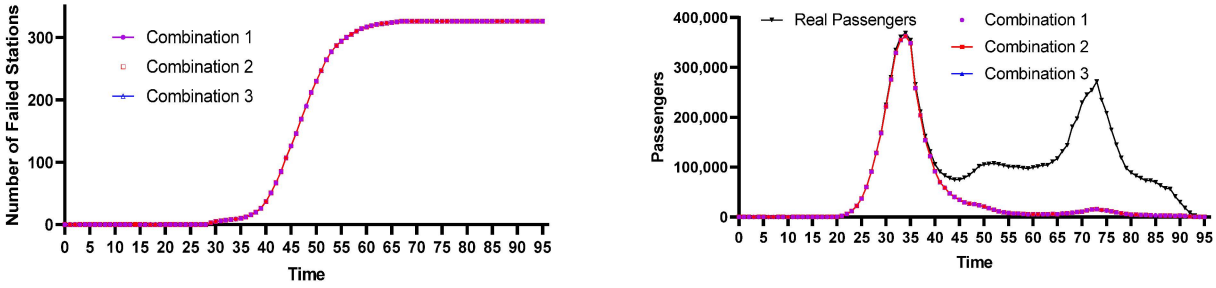

(**a**) (**b**)

Figure 9. (**a**) Cascading failure process under different coupling coefficients of Station 159. (**b**) Passenger flow changes under different coupling coefficients of Station 159.

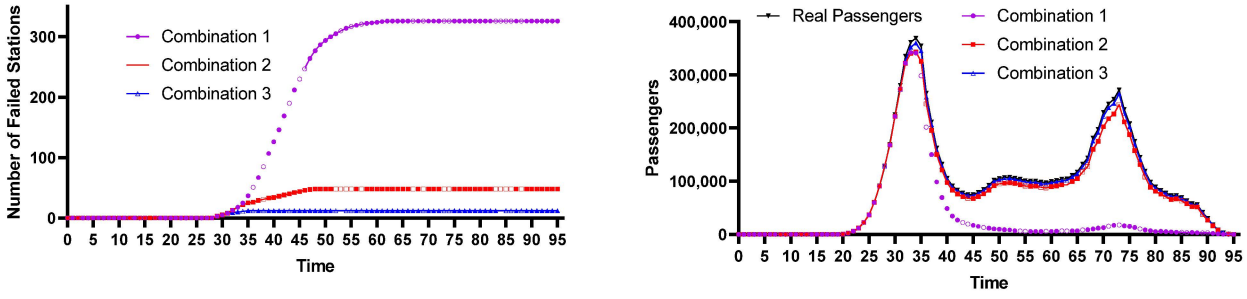

(**a**) (**b**)

Figure 10. (**a**) Cascading failure process under different coupling coefficients of Station 164. (**b**) Passenger flow changes under different coupling coefficients of Station 164.

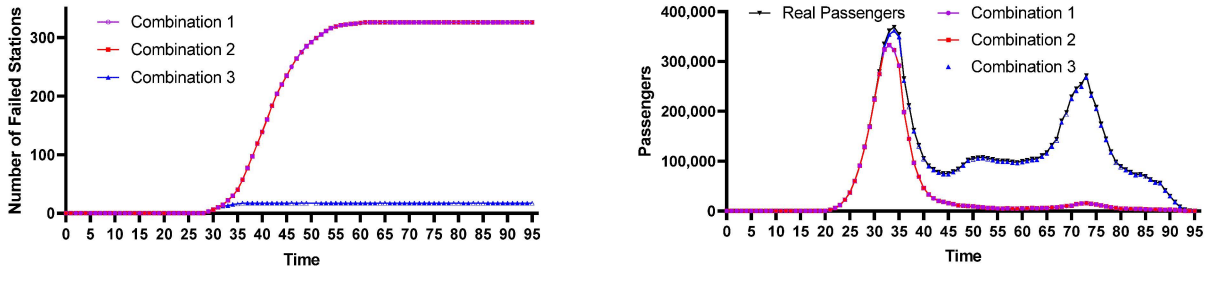

(**a**) (**b**)

Figure 11. (**a**) Cascading failure process under different coupling coefficients of Station 189. (**b**) Passenger flow changes under different coupling coefficients of Station 189.

This study selected three stations with the same depth and degree of centrality to conduct the same experiment, but the overall network damage process varied significantly among the three stations. For Station 159, when the passenger flow coefficient was added (Combination 2) and when both passenger flow and depth coefficients were added (Combination 3), the network damage rate remained the same as when only the degree of centrality was considered (Figure 9a). The entire network's passenger flow would completely cease after the morning peak (Figure 9b).

In the case of Station 164, adding the passenger flow coefficient (Combination 2) slowed down the network damage rate, and most stations remained undamaged at R = 4.

When both passenger flow and depth coefficients were added (Combination 3), the network damage was reduced, with only a dozen stations being destroyed (Figure 10a), and the affected passenger flow was minimal (Figure 10b).

In the experiment with Station 189, adding the passenger flow coefficient (Combination 2) resulted in the same network damage as when only the degree of centrality was considered (Figure 11a). When both passenger flow and depth coefficients were added (Combination 3), similarly to Station 164, the network damage was reduced, with only a dozen stations being destroyed, and the affected passenger flow was minimal (Figure 11b).

4.2.3. Historically Flood-Prone Stations

Given the numerous conditions that can lead to flood disasters, this study focuses on stations that have experienced such events in the past. Three stations were selected for analysis: Shanghai Rail Transit Station 48, which experienced flooding in 2005 (degree of centrality 4, depth 0.87); Station 104, which was suspended during a flood event in 2019 (degree of centrality 4, depth 0.71); and Station 197, which experienced water ingress in 2021 (degree of centrality 4, depth 0.98). The same disturbance, R = 4, was applied under different combinations of coupling coefficients, and the resulting network station damage process and reliability changes are shown in Figures 12–14.

This study examines three stations that have been affected by flood disasters at different times. Although these stations share the same degree of centrality, they differ in depth, leading to significant variations in the overall network damage process. For Station 48, adding the passenger flow coefficient (Combination 2) slowed the overall network damage rate, and the number of damaged stations decreased. When both passenger flow and depth coefficients were added (Combination 3), most stations remained undamaged at R = 4 (Figure 12a), and the impact on passenger flow was minimal (Figure 12b).

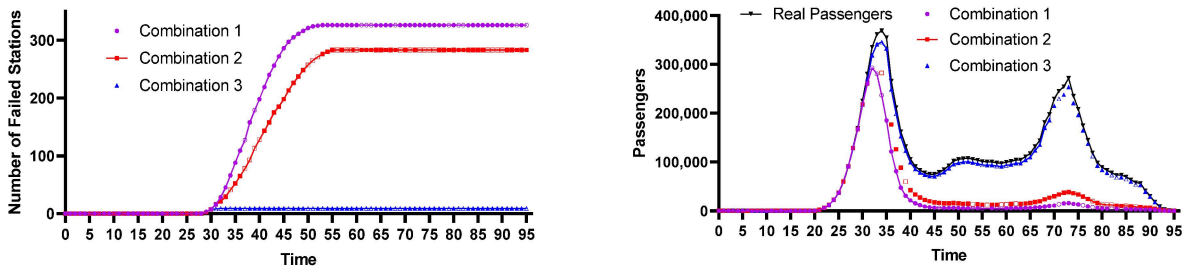

(**a**) (**b**)

Figure 12. (**a**) Cascading failure process under different coupling coefficients of Station 48. (**b**) Passenger flow changes under different coupling coefficients of Station 48.

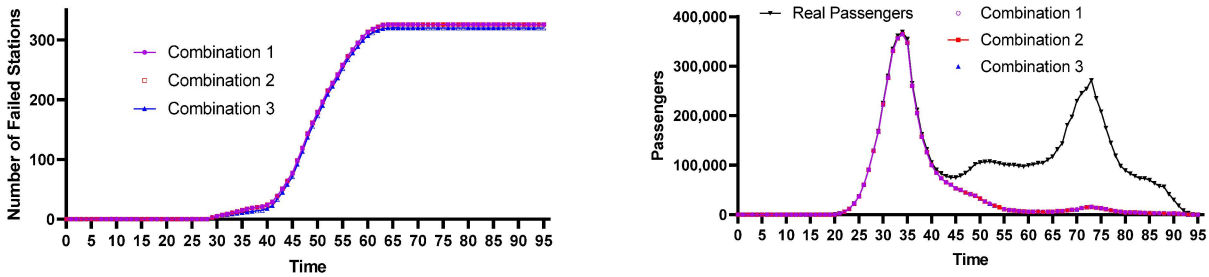

(**a**) (**b**)

Figure 13. (**a**) Cascading failure process under different coupling coefficients of Station 104. (**b**) Passenger flow changes under different coupling coefficients of Station 104.

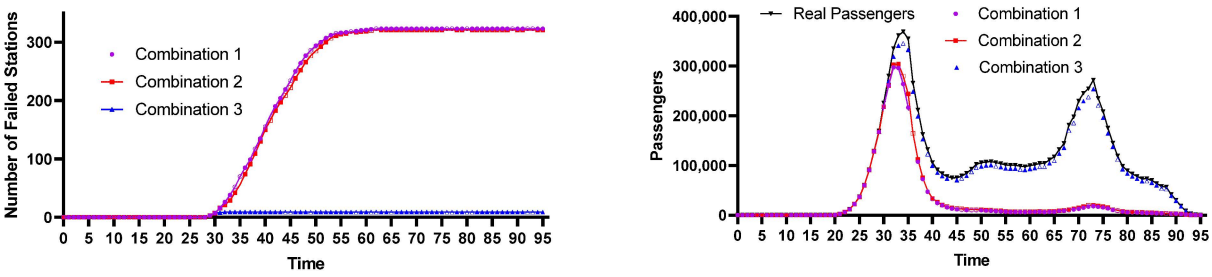

(**a**) (**b**)

Figure 14. (**a**) Cascading failure process under different coupling coefficients of Station 197. (**b**) Passenger flow changes under different coupling coefficients of Station 197.

For Station 104, the overall network damage rate was similar to when only the degree of centrality was considered, regardless of whether the passenger flow coefficient (Combination 2) or both passenger flow and depth coefficients (Combination 3) were added (Figure 13a). After the morning peak, the network was completely destroyed, rendering it unable to sustain any operational capacity (Figure 13b).

In the experiment with Station 197, adding the passenger flow coefficient (Combination 2) slowed the network damage compared to when only the degree of centrality was considered, but the number of damaged stations increased. When both passenger flow and depth coefficients were added (Combination 3), the overall network damage decreased, with only a dozen stations being destroyed (Figure 14a), and the impact on passenger flow was minimal (Figure 14b).

In real cases, after Station 48 was flooded in 2005, the metro implemented certain measures, such as speed restrictions, and related stations only implemented crowd control measures. In 2021, when a large amount of water flowed into Station 197 due to external construction, the operator's strategy was to close the station temporarily, conduct necessary operations, and reopen it within three hours. However, in the case of Station 104 during the 2019 flood, the strategy was to close the related stations one day in advance, which corresponds to the severity of cascading failure observed in this study.

4.2.4. Comparative Analysis

To better compare the cascading failure effects under the same coupling coefficients for different stations, this study conducted a cross-sectional comparison of nine stations. Figure 15a shows the situation of station failures over time under Combination 1 for different stations. Figure 15b shows the situation under Combination 2, and Figure 15c shows the situation under Combination 3.

Figure 15a illustrates the scenario where the coupling coefficient is only based on the degree of centrality. The selected stations all have a relatively high degree of centrality. According to studies, nodes with a higher degree of centrality tend to lead to faster network failures and more station failures [17,24]. However, Figure 15a shows that the stations where the network fails fastest are Station 19 and Station 48, with degree of centrality values of 6 and 4, respectively. Meanwhile, Station 45, although initially failing quickly, has some stations that remain intact. Therefore, it can be concluded that the degree of centrality does influence the speed of cascading failures in the network, but the overall effect on the network's cascading failures can vary depending on the station's location.

Figure 15b illustrates the combined effect of the degree of centrality and dynamic passenger flow coefficients. When passenger flow weighting is added, the network failure speed is faster than when only the degree of centrality is considered [24]. However, Figure 15b shows that after adding the dynamic passenger flow coefficient, because the passenger flow in this study is a real dynamic flow that changes over time and the assumption is that when a station fails, its passenger flow is considered lost and is no longer counted in the network, the impact of the passenger flow diminishes as more stations fail. This results

in fewer station failures (e.g., Stations 164, 19, and 48) and slower failure speeds compared to Figure 15a. Thus, it can be concluded that compared to other all-or-nothing passenger flow indicators, the presence of stations with low overall passenger flows or diminishing passenger flows during failures can slow down the overall cascading failure speed of the network.

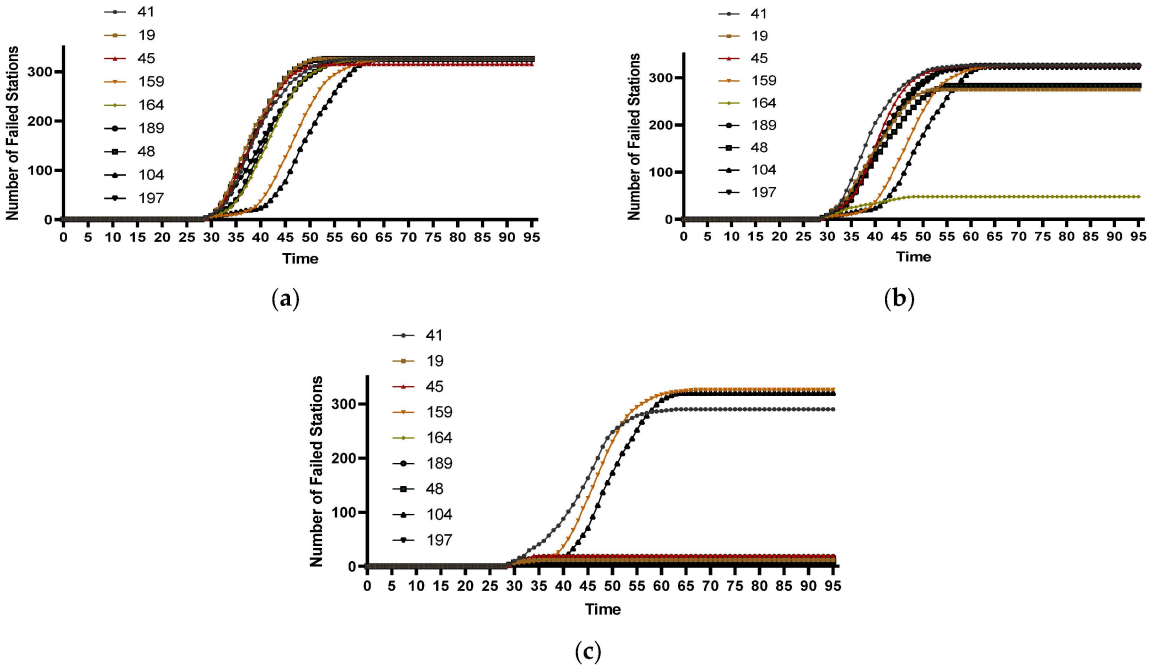

Figure 15. Cascading failure process under (**a**) Combination 1, (**b**) Combination 2, and (**c**) Combination 3 after the failure of different stations.

Figure 15c illustrates the combined effect of the degree of centrality, dynamic passenger flow coefficients, and station elevation coefficients. The results show that after adding the elevation coefficient, as more stations fail, the overall network failure speed slows down, and fewer stations are affected (e.g., Stations 19, 45, 164, 189, 48, and 197). However, there are also instances where the failure speed increases and more stations are affected (e.g., Stations 41, 159, and 104).

4.2.5. Critical Node Failure Analysis and System Vulnerability

This section presents an analysis of key node failures within the urban rail transit network under flood conditions, examining how cascading failures propagate across the system. By evaluating certain factors, such as the degree of centrality, geographic elevation, and dynamic passenger flow, we explore how different scenarios—represented by coupling coefficients C1, C2, and C3—affect the system's vulnerability and overall resilience. The results in Table 1 outline the behavior of critical stations under these varying conditions.

The table illustrates how different combinations of these coefficients influence station behavior. C1 focuses solely on the degree of centrality, C2 integrates dynamic passenger flow, and C3 adds geographic elevation as an additional resilience factor. By incorporating these varying coefficients, we can assess how well these stations resist cascading failures and identify those most vulnerable under flood conditions.

A Failure Mode, Effects, and Criticality Analysis (FMECA) framework is employed to analyze the potential failure modes of key stations and their criticality in the context of system-wide cascading failures. The analysis helps to understand the impact of failures on the entire network, providing insights into which stations are most susceptible to failure and how their failure could propagate through the system.

Table 1. Characteristics of stations and cascading failure sequence.

Station Characteristics			Order of Station Failures			Order of Passenger Flow Impact			Order of Cascading Failure Speed		
Station No.	**Degree**	**Deep**	**C1**	**C2**	**C3**	**C1**	**C2**	**C3**	**C1**	**C2**	**C3**
41	7	0.96	1	1	3	1	1	3	4	1	3
19	6	0.96	1	4	6	1	4	6	1	5	6
45	6	0.93	3	1	4	3	1	4	3	2	4
159	4	0.99	1	1	1	1	1	1	8	7	1
164	4	0.99	1	5	6	1	5	6	7	9	6
189	4	0.99	1	1	5	1	1	5	6	3	7
48	4	0.87	1	3	7	1	3	7	2	7	8
104	4	0.71	1	1	2	1	1	2	9	8	2
197	4	0.98	2	2	7	2	2	7	5	4	8

Stations like 41 and 45, which have a high degree of centrality, exhibit early failures in the C1 and C2 scenarios due to their strong interconnectedness with other parts of the network. Under these conditions, their failure significantly impacts passenger flow, leading to rapid propagation of cascading failures. However, when the geographic elevation coefficient is introduced in C3, the sequence of failures is delayed, thus reducing the speed and extent of the cascading process. This finding demonstrates the importance of incorporating elevation as a resilience factor to mitigate the vulnerability of these key nodes.

In contrast, Stations 159 and 164, which are characterized by lower degrees of centrality but are situated in areas with low elevation, fail early in all scenarios, indicating their high vulnerability to flooding. Although the cascading process is slowed down when additional coefficients are added in C2 and C3, these stations still remain critical points of failure within the network. The persistent vulnerability of these stations suggests that geographic elevation plays a pivotal role in shaping the network's response to flooding events, highlighting the need for targeted infrastructure improvements, such as enhanced flood defenses and drainage systems.

For stations like Stations 48 and 104, although they exhibit lower degrees of centrality, they fail rapidly under C1, particularly in areas with historical exposure to flooding. However, when passenger flow and elevation factors are considered in C2 and C3, the cascading failure process is significantly slowed, further demonstrating the importance of adopting multidimensional approaches in failure analysis.

The results of the FMECA analysis reveal that focusing solely on the degree of centrality does not provide a complete picture of the system's vulnerability. The integration of geographic elevation and passenger flow data is essential to fully capture the dynamics of cascading failures. Stations that are critical due to their centrality and location within the network must be prioritized for infrastructure upgrades and disaster preparedness measures. Improving flood protection at these critical nodes, such as installing better drainage systems or enhancing flood barriers, can help prevent widespread disruptions and ensure network resilience.

Additionally, the incorporation of real-time passenger flow data and geographic factors into emergency response plans can provide transit operators with the tools to better manage failures and optimize evacuation routes. Such proactive measures will help minimize the impact of cascading failures and improve the overall resilience of urban rail transit networks.

In conclusion, the FMECA-based analysis highlights the necessity of considering multiple factors—the degree of centrality, geographic elevation, and passenger flow—when assessing the resilience of urban rail transit systems. By identifying key failure modes and their effects on the network, this analysis provides valuable recommendations for improving system robustness, particularly in flood-prone areas.

5. Conclusions

This study systematically investigates the cascading failure mechanisms and resilience of urban rail transit networks under flood conditions, with a specific focus on the Shanghai Metro. By integrating three-dimensional geographic information, static network characteristics, and dynamic passenger flow data, this research offers a comprehensive framework for evaluating the resilience of urban rail transit systems. The use of the improved CML model allows for a detailed simulation of cascading failure processes, thus providing new insights into the interplay between network topology, geographic factors, and passenger dynamics during flood events.

The findings have significant practical implications for urban transit authorities and disaster management agencies, not only for Shanghai but also for other flood-prone cities globally. The identification of critical nodes within the rail network, which are highly susceptible to cascading failures, offers a foundation for prioritizing infrastructure upgrades and targeted disaster preparedness efforts. By applying these findings, other cities can optimize infrastructure investments in flood-prone areas. For example, increasing drainage capacity or enhancing protection at critical stations could reduce floods' impacts on metro systems. This approach is applicable to cities facing similar risks, thus contributing to a globally relevant disaster management strategy.

Additionally, the dynamic analysis of passenger flow under various flood scenarios provides actionable insights into optimizing evacuation routes and improving emergency response strategies. Incorporating geographic elevation as a resilience indicator highlights the importance of three-dimensional urban topography in the planning and management of urban rail systems. These findings can also be adapted to enhance the robustness of rail networks in other cities vulnerable to floods, making this framework valuable for urban planners and transit operators worldwide.

While previous studies have predominantly focused on static network characteristics and two-dimensional analyses, this research advances the field by integrating real-time data and three-dimensional geographic considerations. By bridging the gap between theoretical modeling and practical applications, this study offers both critical contributions to academic discourse and practical tools for real-world disaster management. The inclusion of geographic factors and passenger dynamics in the improved CML model makes this approach highly adaptable to different urban contexts and disaster scenarios.

However, several areas warrant further investigation. Future research could explore the integration of more sophisticated flood simulation models to account for varying flood intensities and durations. Incorporating real-time data analytics and machine learning algorithms, such as deep learning and reinforcement learning, would enhance the predictive capabilities of the model, thus enabling real-time monitoring and adaptive responses during actual flood events. Expanding the study to include multi-modal transportation networks, such as buses and ferries, could provide a more comprehensive view of urban mobility resilience under extreme weather conditions. Lastly, developing region-specific resilience indicators would tailor disaster response strategies to the unique geographic and infrastructural characteristics of different cities.

In conclusion, this research contributes to the field of urban transportation resilience by offering a novel methodological approach that can be adapted to various contexts. The integration of three-dimensional geographic data with dynamic passenger flow analysis offers a more complete understanding of how urban rail networks respond to flood events. By identifying critical vulnerabilities and offering insights for infrastructure optimization, this study lays the groundwork for more effective disaster response strategies and the development of more resilient urban rail systems globally.

Author Contributions: Conceptualization, D.L. and S.D.; methodology, D.L.; formal analysis, D.L. and Y.H.; data curation, S.D.; writing—original draft preparation, D.L.; writing—review and editing, D.L., Y.H., and F.Z.; supervision, S.D.; project administration, D.L.; funding acquisition, D.L. All authors have read and agreed to the published version of the manuscript.

Funding: This research was funded by Liaocheng University grant number 318051531.

Data Availability Statement: The data presented in this study are available from the corresponding author upon request. The data are not publicly available due to the inclusion of site geographic information.

Conflicts of Interest: The authors declare no conflicts of interest.

References

1. Hurricane Sandy Rebuilding Task Force. *Hurricane Sandy Rebuilding Strategy*; U.S. Department of Housing and Urban Development: Washington, DC, USA, 2013.
2. Watson, G.; Ahn, J.E. A systematic review: To increase transportation infrastructure resilience to flooding events. *Appl. Sci.* **2022**, *12*, 12331. [CrossRef]
3. Bo, K.; Yang, Z.; Lai, X.; Teng, J. Method for identifying the emergency points of urban transit networks in rainstorms with road waterlogging. *J. Transp. Eng. Inf.* **2021**, *20*, 57–67. [CrossRef]
4. Wang, G.; Liu, Y.; Hu, Z.; Zhang, G.; Liu, L.Y. Flood risk assessment of subway systems in metropolitan areas under land subsidence scenario: A case study of beijing. *Remote Sens.* **2021**, *13*, 637. [CrossRef]
5. Li, H.; Ou-Yang, Z.; Jiang, J.; Yang, Q.; Liu, B.; Xi, Y. Urban rail transit disaster chain evolution network model and its risk analysis —Taking subway flood as an example. *Railw. Stand. Des.* **2020**, *64*, 153–157. [CrossRef]
6. Wang, W.; Yang, S.; Stanley, H.E.; Gao, J. Local floods induce large-scale abrupt failures of road networks. *Nat. Commun.* **2019**, *10*, 2114. [CrossRef]
7. Kim, J.; Lee, J.-M.; Kang, J. Smart Cities and Disaster Risk Reduction in South Korea by 2022: The Case of Daegu. *Heliyon* **2023**, *9*, e18794. [CrossRef]
8. Catelani, M.; Ciani, L.; Guidi, G.; Patrizi, G. Maintainability Improvement Using Allocation Methods for Railway Systems. *Acta IMEKO* **2020**, *9*, 10–17. [CrossRef]
9. Khaliq, K.A.; Chughtai, O.; Shahwani, A.; Qayyum, A.; Pannek, J. An Emergency Response System: Construction, Validation, and Experiments for Disaster Management in a Vehicular Environment. *Sensors* **2019**, *19*, 1150. [CrossRef]
10. Kumsap, C.; Sinnung, S.; Boonthalarath, S. Establishing a Mesh Communication Backbone for Disaster Management: Proof of Concept. In Proceedings of the 9th International Defense and Homeland Security Simulation Workshop (DHSS 2019), Lisbon, Portugal, 18–20 September 2019; pp. 10–15.
11. Lagap, U.; Ghaffarian, S. Digital Post-Disaster Risk Management Twinning: A Review and Improved Conceptual Framework. *Int. J. Disaster Risk Reduct.* **2024**, *110*, 104629. [CrossRef]
12. De Francesco, E.; Leccese, F. Risks Analysis for Already Existent Electric Lifelines in Case of Seismic Disaster. In Proceedings of the 2012 11th International Conference on Environment and Electrical Engineering (EEEIC 2012), Venice, Italy, 18–25 May 2012; pp. 830–834.
13. Zhang, D.; Yin, J.; Zhu, X.; Zhang, C. Network representation learning: A survey. *IEEE Trans. Big Data* **2018**, *6*, 3–28. [CrossRef]
14. Yin, D.; Huang, W.; Shuai, B.; Liu, H.; Zhang, Y. Structural characteristics analysis and cascading failure impact analysis of urban rail transit network: From the perspective of multi-layer network. *Reliab. Eng. Syst. Saf.* **2022**, *218*, 108161. [CrossRef]
15. Du, F.; Huang, H.; Zhang, D.; Zhang, F. Analysis of characteristics of complex network and robustness in Shanghai metro network. *Eng. J. Wuhan Univ.* **2016**, *49*, 701–707. [CrossRef]
16. Yang, J.; Zhu, D.; Zhao, R. Analysis on characteristics of urban rail transit network and robustness of cascading failure. *Comput. Eng. Appl.* **2022**, *58*, 250–258. [CrossRef]
17. Li, S.; Shuai, B.; Liu, Y. Cascading failure mechanism of urban rail transit network. *China Transp. Rev.* **2020**, *42*, 69–74+120.
18. Hu, J.; Yang, M.; Zhen, Y. A review of resilience assessment and recovery strategies of urban rail transit networks. *Sustainability* **2024**, *16*, 6390. [CrossRef]
19. Mabrouk, M.; Han, H.; Mahran, M.G.N.; Abdrabo, K.I.; Yousry, A. Revisiting urban resilience: A systematic review of multiple-scale urban form indicators in flood resilience assessment. *Sustainability* **2024**, *16*, 5076. [CrossRef]
20. Dehmamy, N.; Milanlouei, S.; Barabási, A.L. A structural transition in physical networks. *Nature* **2018**, *563*, 676–680. [CrossRef]
21. Chen, F.; Hu, Y.; Li, X.; Chen, P. Cascading failures in weighted network of urban rail transit. *J. Transp. Syst. Eng. Inf. Technol.* **2016**, *16*, 139–145. [CrossRef]
22. Liu, Z.; Lu, Y.; Liu, B.; Li, Q.; Lu, W. Cascading Failure resistance of urban rail transit network. *J. Transp. Syst. Eng. Inf. Technol.* **2018**, *18*, 82–87. [CrossRef]
23. Huang, A.; Wu, X.; Guan, W.; Duan, M. Evolution of metro network stability based on weighted coupled map lattice. *J. Transp. Syst. Eng. Inf. Technol.* **2021**, *21*, 140–149. [CrossRef]
24. Zhu, Y.; Sun, J.; Wang, X. Reliability analysis of urban rail transit system network based on coupled map lattice model. *J. Univ. Shanghai Sci. Technol.* **2021**, *43*, 93–101. [CrossRef]
25. Ye, H.; Luo, X. Cascading failure analysis on shanghai metro networks: An improved coupled map lattices model based on graph attention networks. *Int. J. Environ. Res. Public Health* **2021**, *19*, 204. [CrossRef] [PubMed]
26. Feng, S.; Wang, S.; Zhao, H. Cascading failure analysis of urban rail transit network based on coupled map lattice model. In Proceedings of the CICTP 2020, Xi'an, China, 14–16 August 2020; pp. 2074–2084.

27. Shen, Y.; Ren, G.; Ran, B. Cascading failure analysis and robustness optimization of metro networks based on coupled map lattices: A case study of Nanjing, China. *Transportation* **2019**, *48*, 537–553. [CrossRef]
28. Ma, Z. The impact of passenger behavior on urban rail transit network failure. *Urban Rail Transit Stud.* **2022**, *25*, 225–232.
29. Li, P.; Xu, Z.; Zhao, G.; Zuo, B.; Wang, J.; Song, S. Simulation of urban rainstorm waterlogging process based on SWMM and LISFLOOD-FP models-Case study in Jinan City. *South-North Water Transf. Water Sci. Technol.* **2021**, *19*, 1083–1092. [CrossRef]